Adsorption isotherm, kinetic and mechanism studies of crystal violet dye by activated carbon from sugarcane leaves

Suchada Sawasdee and Prachart Watcharabundit*

Department of Chemistry, Faculty of Science and Technology, Thepsatri Rajabhat University
Email: prachartw@hotmail.com
Received: November 09, 2021; Revised: December 13, 2021; Accepted: December 15, 2021

Abstract

In this study, the activated carbon was prepared from sugarcane leaves under the chemical activation with NaCl for the adsorption of crystal violet dye in an aqueous solution. The effect of various experimental parameters, such as pH (2-10), contact time (10-420 min), initial dye concentration (25-300 mg/L), and temperature (20, 30, and 40°C) was investigated. The adsorbent was characterized by Fourier transform infrared spectroscopy (FTIR). The results showed that the equilibrium adsorption data were better described by the Langmuir than the Freundlich and Dubinin–Radushkevich isotherm models, and the maximum adsorption capacity was found to be 9.47 mg/g at 30°C. The adsorption kinetics agreed well with the pseudo-second-order model. Thermodynamically, the process was spontaneous and endothermic. The mechanisms of crystal violet adsorption onto activated carbon were an electrostatic attraction, hydrogen bonding, Yoshida hydrogen bonding, and n-π interaction.

Keywords: Adsorption, crystal violet, activated carbon, sugarcane leaves, mechanism

1. Introduction

Dyes are used for dying products (textiles, paper, plastic, leather, food, and cosmetics, etc.), and they are lost in dye effluent during such a dying process. In addition, the stability of most dye molecules under the condition of light, heat, and chemicals leads to the fact that the dying effluents are difficult to degrade [1]. The presence of dyes can cause damage to living beings in the water.

Crystal violet, used as a commercial textile dye, is a recalcitrant molecule that is poorly metabolized by microbes and consequently is long-lived in the environment [2]. It is carcinogenic and non-biodegradable and can persist in various environments [3]. It is harmful by inhalation, ingestion through skin contact and has been found to cause cancer, severe eye irritation in human beings [4].

Several treatments have been used to remove dyes from aqueous solutions. Among several dye removal techniques, adsorption is efficient in removing different kinds of dyes from water and wastewater. Activated carbon is the most efficient adsorbent because of its high surface area, but it is relatively high. Therefore, much attention is on preparing activated carbon from agricultural waste for ultimate use as adsorbents [5, 6].

Sugarcane bagasse offers a large amount of sugarcane leave waste. Sugarcane leaves left in the fields during sugarcane harvesting are burnt, which produces fly ash, severely damages soil microbial diversity, and raises environmental concerns. Many studies have been conducted to search for the sugarcane-leaf biomass for wastewater treatment such as Pb(II) [7], Pb(II), Cd(II), and Cr [8], Ni(II), Cr(III) and Co(II) [9], Auramine-O [10], and methyl orange [11]. However, there have been no research reports on removing crystal violet dye with sugarcane-leaf-activated carbon.

In this work, sugarcane leaves were used to prepare activated carbon and applied for crystal violet removal in an aqueous solution under the batch adsorption process. The activated carbon was characterized by Fourier transform infrared analysis (FTIR). The various adsorption parameters, such as pH, contact time, initial dye concentration, and temperature, were investigated. The experimental data were analyzed by isotherm and kinetic models. Also, the thermodynamic study was evaluated. Then, the adsorption mechanism was presented.

1.1 Preparation of adsorbent

Sugarcane leaves were obtained from Khok Samrong District, Lopburi, Thailand. They were washed several times with tap water and dried in a hot air oven. Then, sugarcane leaves were cut to about 1 inch and soaked in 2.0 M sodium chloride with a ratio of 1:20 (g/ml) for 24 hr. It was dried at a temperature of 100ºC for 24 hr. The char of sugarcane leaves was heated up to activation temperature at 400ºC for 2 hr. After that, it was rinsed with distilled water until its pH value was 7. The activated carbon from sugarcane leaves (ACSL) was dried at 100°C and crushed with a blender, and sieved particle size to 150-300 μm. Then, it was stored in a desiccator until used.

1.2 Preparation of adsorbate

APS Ajax Finechem, Australia supplied crystal violet (C.I.42555, chemical formula, $C_{25}H_{20}ClN_3$, molecular weight = 407.99 g mol^{-1}), and its molecular structure is shown in Fig 1. Adsorbate was dried at 80°C for 2 h. [12].

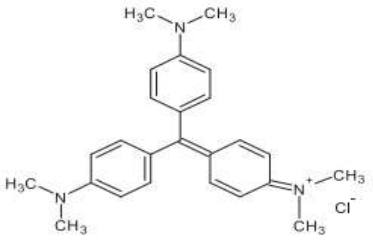

Figure 1. Structure of crystal violet

1.3 Characterization of adsorbent

The adsorbent was characterized by Fourier transform infrared analysis (FTIR, Perkin Elmer, model two) in the range of 4000 to 400 cm^{-1}.

2. Batch of dye adsorption

For the adsorption experiment, the effect of parameters, such as pH (2-10), contact time (10-420 min), and dye concentration (25-300 mg/L), was investigated. In each experiment, 100 ml of crystal violet solution was added to 1.0 g of activated carbon in a 250-ml Erlenmeyer flask. The flasks of the mixture were stirred at 200 rpm in an isothermal shaker. At the end of adsorption at any time, the sample was filtered, and the dye concentration remaining in the solution was measured by a double beam UV-Visible spectrophotometer at 585 nm.

The percentage (%) and the amount of adsorption, q_t (mg/g) were calculated by equations (1) and (2):

$$\% \text{ adsorption} = \frac{(C_o - C_e)\times 100}{C_o} \quad (1)$$

$$q_t = \frac{(C_o - C_t)V}{W} \quad (2)$$

where C_o (mg/L) is initial dye concentration, C_t (mg/L) is the concentration at any time, q_t (mg/g) is the amount adsorbed at any time, V(L) is the volume of the solution and W(g) is the mass of adsorbent. Each experimental treatment was run in triplicate.

2.1 Adsorption Isotherm

. The Langmuir isotherm in a linear form is represented as follows [3]:

$$\frac{C_e}{q_e} = \frac{1}{q_{max}} C_e + \frac{1}{K_L q_m} \quad (3)$$

where C_e (mg/L) is the equilibrium concentration, q_e (mg/g) is the amount adsorbed at equilibrium, K_L is the Langmuir constant, and q_{max} (mg/g) is the maximum adsorption capacity. The essential characteristics of a Langmuir isotherm can be expressed in terms of a dimensionless separation factor (R_L) which is defined by:

$$R_L = \frac{1}{(1+K_L C_o)} \quad (4)$$

The Freundlich isotherm in a linear form is represented as follows [3]:

$$\log q_e = \log K_F + \frac{1}{n} \log C_e \quad (5)$$

where K_F (L/g) is the adsorption capacity and $\frac{1}{n}$ is the adsorption intensity [3].

The Dubinin–Radushkevich isotherm in a linear form is represented as follows [3]:

$$\ln q_e = \ln q_o - K_{DR}.\varepsilon^2 \quad (6)$$

where ε can be correlated in Equation (7):

$$\varepsilon^2 = [RT \ln (1+1/C_e)]^2 \quad (7)$$

The constant K_{DR} gives an idea about the mean adsorption energy (E, kJ/mol), which explain the adsorption mechanism, and the equation is shown as follows:

$$E = \frac{1}{\sqrt{2K_{DR}}} \quad (8)$$

2.2 Adsorption Kinetics

The pseudo-first-order kinetic in a linear form is written as follows [4]:

$$\log (q_e - q_t) = \log q_e - \frac{k_1}{2.303} t \quad (9)$$

where k_1 (min^{-1}) is the rate constant of pseudo-first-order, and q_t (mg/g) is the amount adsorbed at any time (min).

The pseudo-second-order kinetic in a linear form is written as follows [4]:

$$\frac{t}{q_t} = \frac{1}{k_2 q_e^2} + \frac{1}{q_e} t \qquad (10)$$

where k_2 ($g.mg^{-1}.min^{-1}$) is the rate constant of pseudo-second-order kinetic adsorption.

The intraparticle diffusion model is written as follows:

$$q_t = K_{id}(t)^{1/2} + C \qquad (11)$$

where K_{id} is the intraparticle diffusion rate constant ($mg/(g.min^{1/2})$), and C gives the idea of the thickness of the boundary layer.

3. Results and discussion

3.1 FTIR study

FTIR spectra of ACSL before and after dye adsorption are shown in Fig 1. Prior to the adsorption, the broad band observed in the range of 3,200-3,500 cm^{-1} belongs to the hydroxyl O-H group [13]. The peaks in the region of 2,850-3,000 cm^{-1} indicate the presence of C-H stretching vibration [14]. The peaks observed in the range of 1,600-1,820 cm^{-1} indicate the presence of C=O groups [13], The adsorption peaks of C=O in the carboxylic acid and ketone appear at 1714.28$cm^{-1}$and 1676.94 cm^{-}1, respectively. The peak at 1579.13 cm^{-1} indicates probable C=C stretching in aromatic rings [15, 16]. The peaks observed in the range of 1,300-1,420 cm^{-1} referred to C = C-H in-plane bending suggesting several bands in cellulose and xylose [17]. In addition, the peak at 1259.79 cm^{-1} results from C-O stretching vibration in lignin and xylan [18]. Meanwhile, the FTIR peak at 1101.02 cm^{-1} is related to the stretching C-O group [19]

After adsorption, the FTIR bands are shifted because of the interaction of CV molecules at the functional groups of the activated carbon.

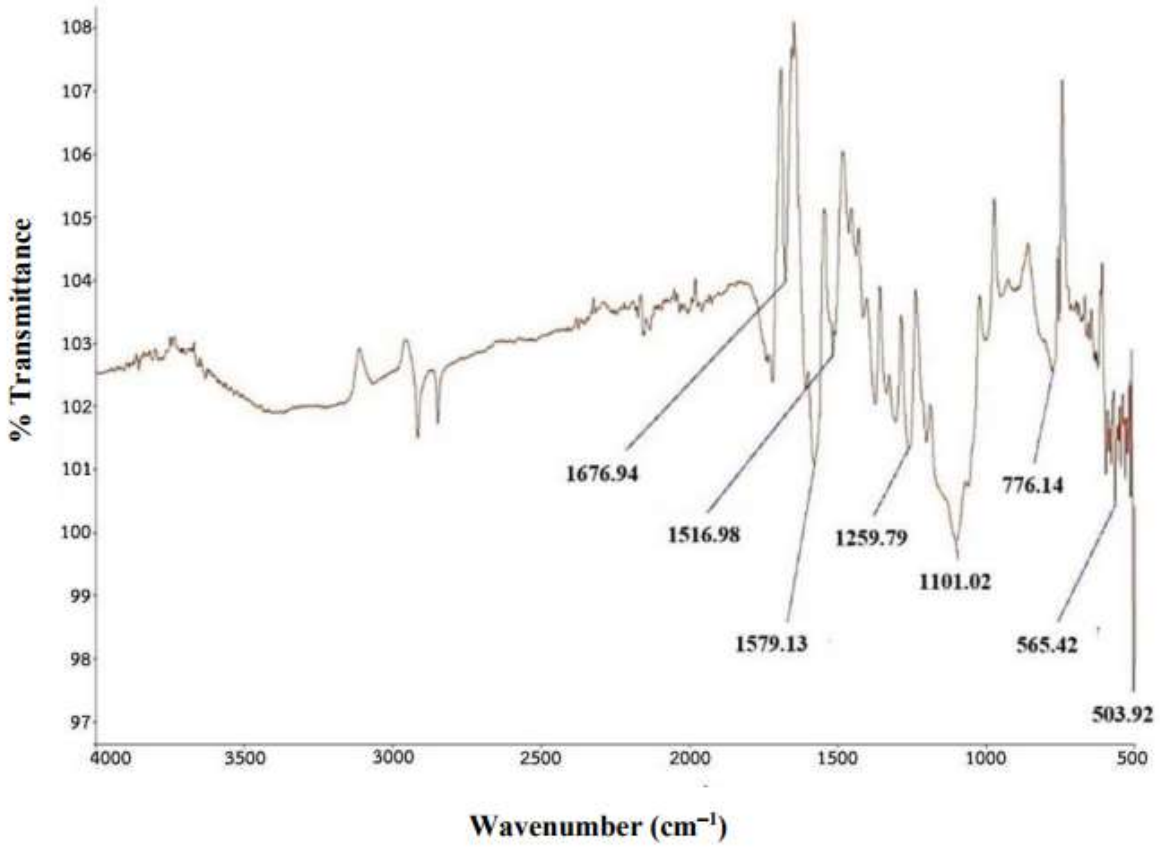

(a) ACSL before adsorption

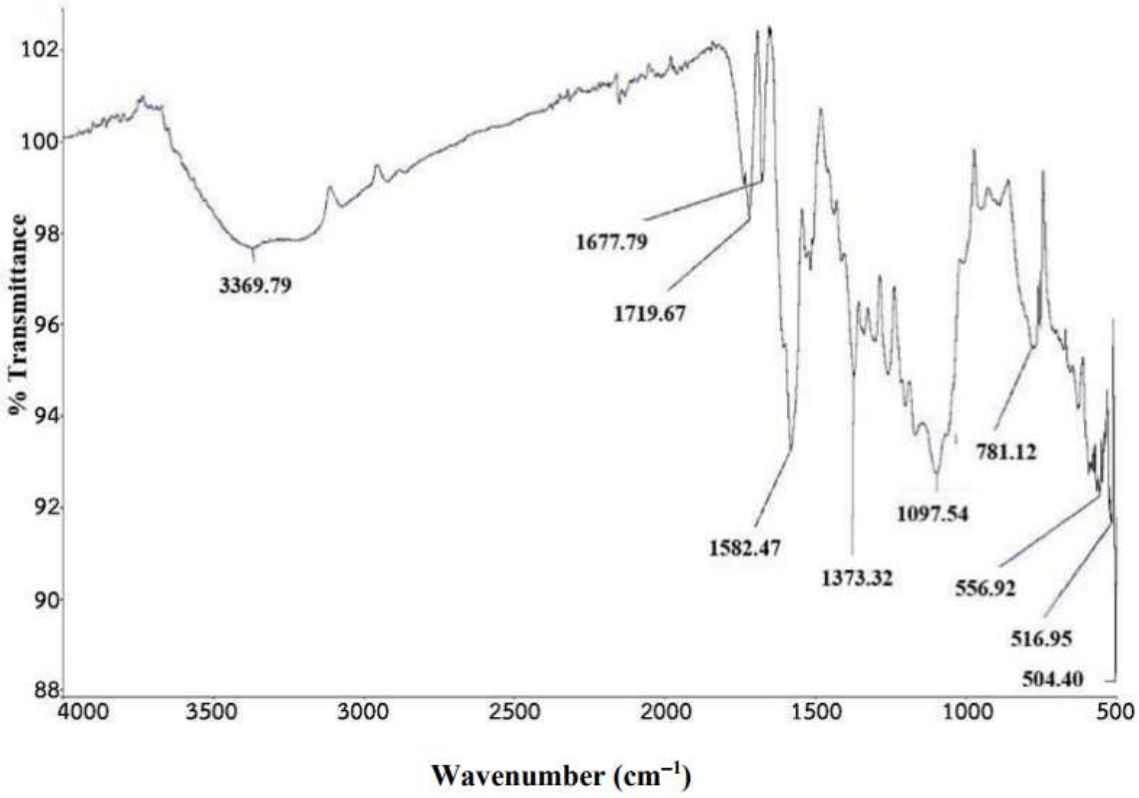

(b) ACSL after adsorption

Figure 1. **FTIR of adsorbent (a) before adsorption and (b) after adsorption**

3.2 Effect of pH

The effect of pH is an essential factor for the adsorption process. It was found that the removal of CV increased with increasing pH, as shown in Fig. 2. The maximum dye removal was observed at pH 8 (90.67%).

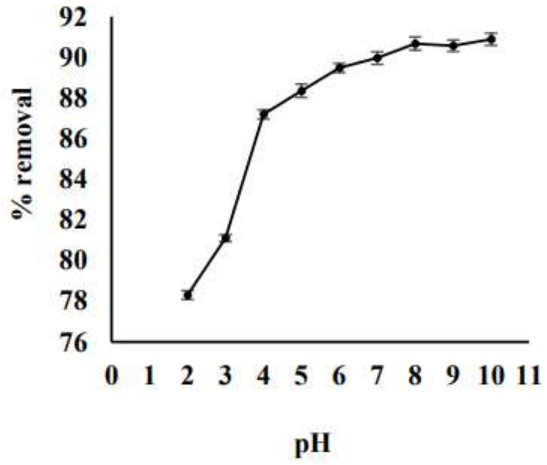

Figure 2 Effect of pH (initial CV concentration 50 mg/L, dose 1.0 g, temperature 30°C)

At low pH, low adsorption was observed due to the repulsion between CV^+ and positive charge on the adsorbent's surface.

The adsorbent's surface becomes negatively charged at higher pH, increasing adsorption. The adsorption reaction (electrostatic interaction) is shown as follows:

$$R\text{-}OH + OH^- \rightarrow R\text{-}O^- + H_2O \qquad (12)$$

$$R\text{-}O^- + CV^+ \rightarrow R\text{-}O^-\ CV^+ \qquad (13)$$

3.3 Effect of contact time

For the effect of contact time, the adsorption experiments were carried out at varying contact times between 10-480 min, and the adsorption data were shown in Fig 3.

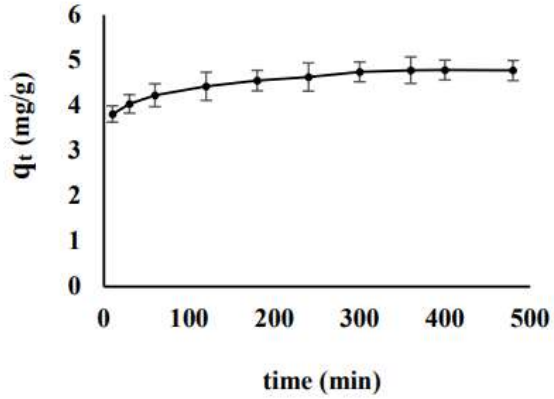

Figure 3 Effect of contact time (pH 8, initial CV concentration 50 mg/L, dose 1.0 g, temperature 30°C)

During the first rapid adsorption stage, dye molecules adsorbed on the external surface of activated carbon via boundary layer adsorption due to the availability of high surface area [20]. As seen in Fig. 3, the $R^2 = 0.992$ adsorption occurred very rapidly in the initial stage of the contact time at 10 min $(q_t = 3.81\text{mg/g})$ and gradually increased with time until it reached the equilibrium at 360 min $(q_t = 4.78\text{mg/g})$ In the second stage, crystal violet passed deeper into the micropores of activated carbon. This diffusion step faced higher resistance as the micropores got filled up, and it caused the process to $R^2 = 0.999$ be slower [21].

3.4 Adsorption kinetics

The adsorption data, obtained from the effect of contact time, were analyzed by three kinetic models. The linear plots of pseudo-first-order, pseudo-second-order, and intraparticle diffusion are shown in Figure 4 (a, b, and c). The result showed that the correlation coefficient (R^2) of the pseudo-second kinetic model $(R^2 = 0.999)$ was more than that of the pseudo-first-order $(R^2 = 0.992)$ Moreover, the $q_e(4.85\text{mg/g})$ value calculated by the pseudo-second-order model was closer to the experimental $q_e(4.78\text{mg/g})$

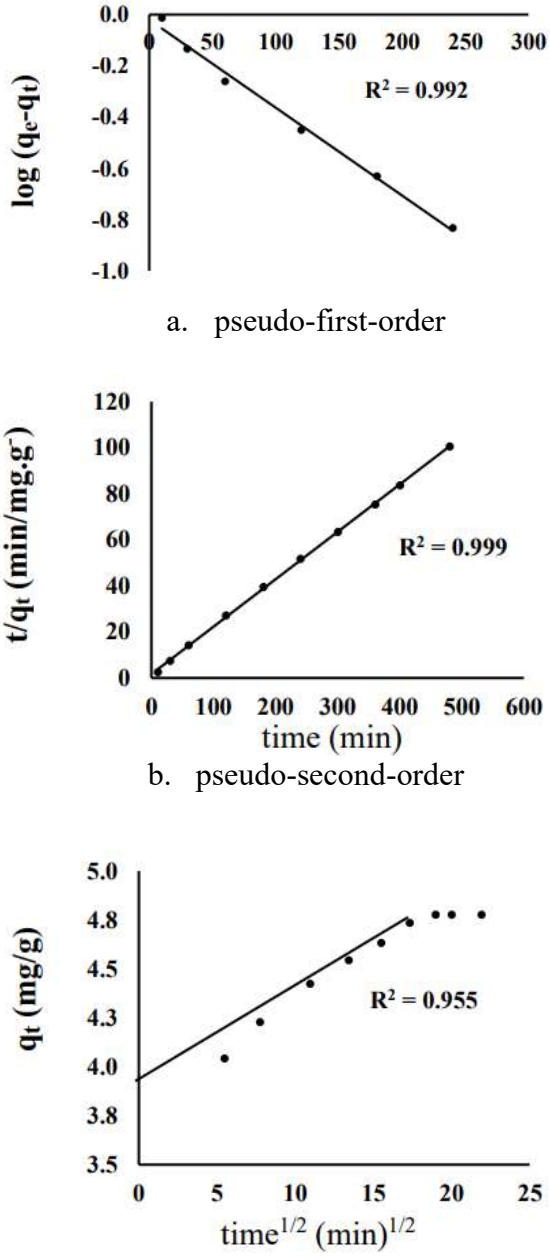

Figure 4 Kinetics of dye adsorption

The data were fitted better to the pseudo-second-order, indicating that the dye adsorption process was an external surface reaction. The kinetic parameters were calculated as shown in Table 1.

For the intraparticle diffusion model (Fig. 4c), it was observed that the plot presented three linear portions, and the straight lines did not pass through the origin, indicating that the intraparticle diffusion was not the only rate-controlling step [22, 23].

Table 1. Kinetics of dye adsorption

Kinetic models	parameters
q_e((exp) (mg/g)	4.78
Pseudo–first order	
q_e(cal) (mg/g)	1.58
k_1 (min^{-1})	2×10^{-3}
R^2	0.992
Pseudo–second order	
q_e(cal) (mg/g)	4.85
k_2 ($g.mg^{-1}.min^{-1}$)	2.6×10^{-2}
R^2	0.999
Intraparticle diffusion	
K_{id}	0.041
C (mg/g)	3.992
R^2	0.955

3.5 Effect of initial concentration of dye

The equilibrium adsorption experiments were investigated at varying initial concentrations (25, 50, 100, 200, and 300 mg/L). In Figure 5, the plot of $q_e$qe against initial concentrations (C_0) is shown.

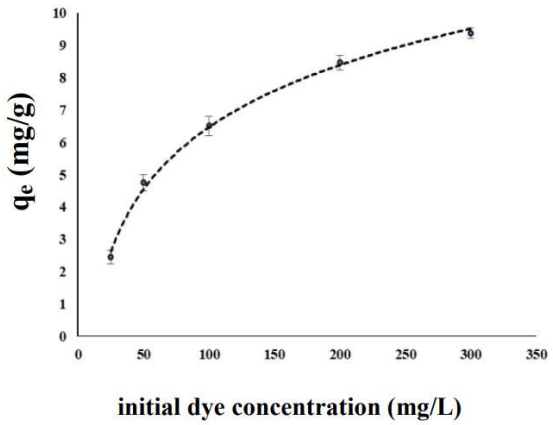

Figure 5. Effect of initial dye concentration (pH 8, dose 1.0 g, time 360 min, temperature 30°C)

The results showed that the equilibrium adsorption capacity (q_e) increased as the initial dye concentration increased and gradually increased after that. This may be due to the increase in the driving force of the concentration gradient for mass transfer with the rise of the initial dye concentration. However, the dye uptake capacity would occur until sorbent saturation was achieved. This was due to a limited number of active sites and pores on the adsorbent [24], and the available surface area of the adsorbent became smaller as CV molecules got adsorbed on the adsorbent surface, resulting in the removing rate gradually slowing downed until reaching saturation at equilibrium.

3.6 Adsorption isotherm

The equilibrium adsorption data of CV on ACSL were tested by the Langmuir, Freundlich, and Dubinin–Radushkevich isotherms. The linear plots of isotherm are shown in Fig 6 (a, b, c), and the corresponding adsorption parameters and the relative coefficients (R^2) are presented in Table 2. According to R^2, the experimental data fit the Langmuir better than the Freundlich and Dubinin–Radushkevich isotherm models.

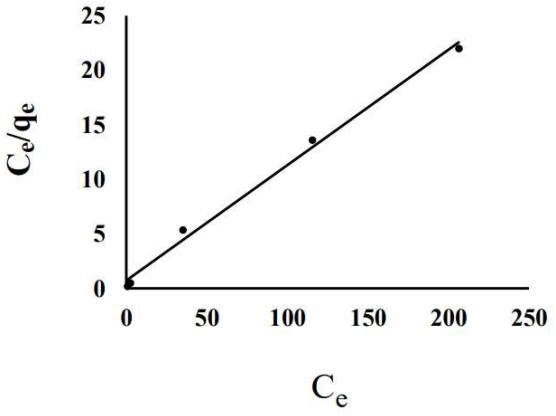

a. Langmuir isotherm

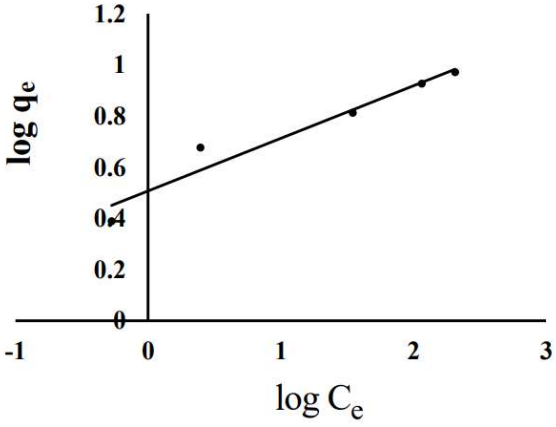

b. Freundlich isotherm

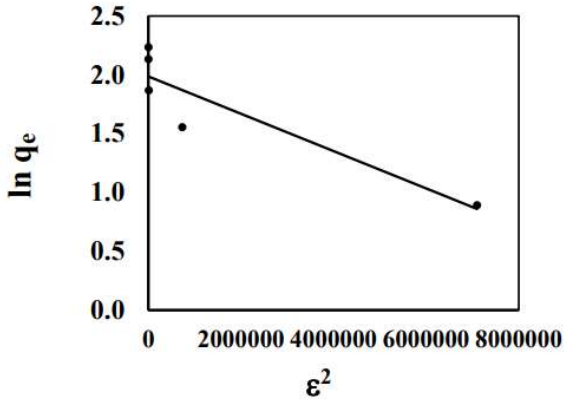

c. Dubinin-Radushkevich isotherm

Figure 6. Isotherm models on adsorption

The Langmuir isotherm confirmed the monolayer coverage of dye on ACSL and the maximum adsorption capacity (q_{max}) was found to be 9.47 mg/g at 30°C. Furthermore, the parameters (R_L) were found in the range of 0-1, confirming the favorable adsorption for CV on ACSL.

Table 2. Isotherm parameters for adsorption of CV on ACSL

Isotherm models	parameters
Langmuir isotherm	
q_{max} (mg/g)	9.47
K_L (L/g)	1.40
R_L	0.028-0.002
R^2	0.993
Freundlich isotherm	
K_F (L/mg)	3.21
1/n	0.20
R^2	0.945
Dubinin–Radushkevich	
q (mg/g)	7.29
E (kJ/mol)	2.23
R^2	0.831

For the Freundlich isotherm, the value of 1/n below 1 indicated a normal Langmuir isotherm and reflected the adsorption was favorable [25].

For the Dubinin–Radushkevich isotherm, the plot of ln q_e versus ε^2 (Figure 6c) enabled the constant K_{DB} and E was determined (Table 2) by Eq. (8). The E value of 2.23 kJ/mol revealed that the adsorption was a physical process, as the magnitude of E was below 8 kJ/mol [26].

3.7 Thermodynamic of adsorption

To evaluate the thermodynamic parameters of adsorption, the adsorption experiments were carried out at 20, 30, and 40°C for initial dye concentration at 50 mg/L, and its plot of log (q_e/C_e) against 1/T is shown in Fig 7.

The thermodynamic parameters of adsorption are shown in Table 3. The values of ΔG were estimated to be –0.296, –1.641, and –3.603 kJ/mol at 20, 30, and 40°C, respectively. The negative value of ΔG indicated that the adsorption was spontaneous and favorable adsorption.

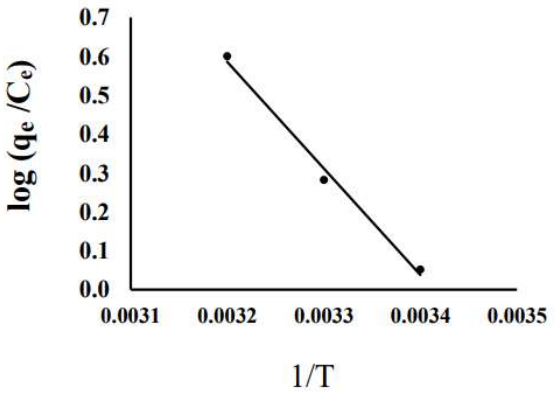

Figure 7. Thermodynamic of adsorption (pH 8, dose 1.0 g, time 360 min.)

Table 3. Thermodynamic parameters of CV adsorption on ACSL

Tem (K)	–ΔG (kJ/mol)	ΔH (kJ/mol)	ΔS (J/mol)
298	0.296	52.507	179.250
303	1.641		
308	3.603		

The positive value of ΔH was 52.507 kJ/mol, indicating that the adsorption was an endothermic process. The positive value of ΔS was 179.250 J/mol, indicating that the adsorption increased randomness at the solid/liquid interface during the adsorption process.

3.8 Mechanism of adsorption

Possible mechanisms of the adsorption are presented in Fig. 8. In alkaline condition at pH 8, the adsorption mechanism was an electrostatic attraction (— · · —) as discussed in section 3.3. By the FTIR study, the oxygen-containing functional groups on activated carbon can form hydrogen bonding (– – – –), Yoshida- hydrogen bonding (·····) and n-π interaction (----------). For after adsorption, FTIR peak at around 3350 cm^{-1} was shifted to 3369.79. This result suggested that hydrogen bonding and Yoshida-hydrogen bonding might be formed. This suggestion was similar to the adsorption of crystal violet onto the almond shell surface [27]. In addition, the C-O peak of the activated carbon decreased its intensity and shifted to a lower wavenumber from 1101.02 to 1097.54 cm^{-1}, confirming the presence of n-π interactions. This finding is consistent with the adsorption of cationic dye on activated charcoal [28].

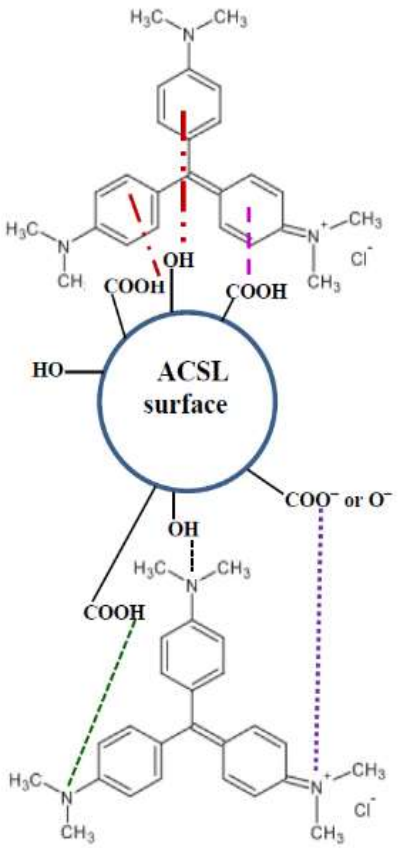

Figure 8. Mechanism of crystal violet dye adsorption on ACSL surface

4. Conclusion

In the present study, the adsorption of crystal violet on activated carbon prepared from sugarcane leaves by NaCl activation was investigated under batch conditions. The adsorption capacity increased with the increase of pH, contact time, initial dye concentration, and temperature. The maximum dye adsorption percentage was 90.67% at pH 8, and adsorption reached equilibrium at 360 min. The experimental data were better described by the Langmuir isotherm. The kinetic adsorption data were best described by the pseudo-second-order model. The intraparticle diffusion study showed that the adsorption was not the only rate-limiting step. The thermodynamic analysis confirmed that the dye adsorption was spontaneous and favorable, and it was endothermic. The adsorption mechanisms of CV on activated carbon were electrostatic attraction, hydrogen bonding, Yoshida hydrogen bonding, and n-π interactions.

5. References

[1] X. Han, X. Niu and X. Ma, "Adsorption characteristics of methylene blue on poplar leaf in batch mode: Equilibrium, kinetics and thermodynamics," Korean Journal of Chemical Engineering, 29(4), pp. 494–502, 2012.

[2] C.C. Chen, H.J. Liao, C.Y. Cheng and Y.C. Chung, "Biodegradation of crystal violet by *Pseudomonas putida,"* Biotechnology Letters, 29, pp.391–396, 2007.

[3] S. Chakraborty, S. Chowdhury and P.D. Saha, "Adsorption of Crystal Violet from aqueous solution onto NaOH-modified rice husk," Carbohydrate Polymers, 86(4), pp. 1533-1541, 2011.

[4] R. Ahmad. "Studies on adsorption of crystal violet dye from aqueous solution onto coniferous pinus bark powder (CPBP)," Journal of Hazardous Materials, 171(1–3), pp.767–773, 2009.

[5] C.A. Basar. "Applicability of the various adsorption models of three dyes adsorption onto activated carbon prepared waste apricot," Journal of

Hazardous Materials, B135, pp. 232–241, 2006.

[6] G. O. El–Sayed, M. M. Yehia and A. A. Asaad. “Assessment of activated carbon prepared from corncob by chemical activation with phosphoric acid,” Water Resources and Industry, 7–8, pp.66–75, 2004.

[7] G.JAREDA and S. P. MAHAPATRA. “Column Adsorption Technique for the Removal of Pb^{+2} ions Using Sugarcane Leave,” ORIENTAL JOURNAL OF CHEMISTRY, 33(6), pp. 3225-3234, 2017.

[8] A. Zahir Hussain and K. M. Mohamed Sheriff. “Removal of heavy metals from wastewater using sugarcane leaf as adsorbent,” Pelagia Research Library, 5(4), pp.56-58, 2014.

[9] Adigun, O. A., Oninla, V. O., Babarinde, N. A. A., Oyedotun, K. O., & Manyala, N. (2020). “Characterization of sugarcane leaf-biomass and investigation of its efficiency in removing Nickel(II), Chromium(III) and Cobalt(II) ions from polluted water,” Surfaces and Interfaces, 20, pp.100621, 2020.

[10] C. Qi , M. Menga , Q. Liub , C. Kanga , S. Huang, Z. Zhou and C. Chen. “Adsorption Kinetics and Thermodynamics of AuramineO on Sugarcane Leaves Based Activated Carbon,” Journal of Dispersion Science and Technology, 36(9), pp.1257–1263, 2014.

[11] G. K. Cheruiyot, W. C. Wanyonyi, Ki. J. Joyce and E. N. Maina. “Adsorption of Toxic Crystal Violet Dye Using Coffee Husks: Equilibrium, Kinetics and Thermodynamics Study,” Scientific African, 5, 2019.

[12] S.MAULINA, G.HANDIKA, Irvan and A. H. ISWANTO. “Quality Comparison of Activated Carbon Produced From Oil Palm Fronds by Chemical Activation Using Sodium Carbonate versus Sodium Chloride, Journal of the Korean Wood Science and Technology. 48(4), pp.503-512, 2020.

[13] G. M. Shah, M. Nasir, M. H. F. Imran, F. Rabbani, M. Sajjad, A. B. U. Farooq and L.Song. “Biosorption potential of natural, pyrolysed and acid-assisted pyrolysed sugarcane bagasse for the removal of lead from contaminated water,” PeerJ, 6, 2018.

[14] S. Wang, TL. Li, P. Yi and JJ. Yuan “Modified phoenix tree leaves and their adsorption removal of Ca^{2+} from wastewater.” ScienceAsia 47: 1-8, 2021. Doi:10.2306/scienceasia15131874.2021.061

[15] M.R. Kulkarni, T. Revanth, A. Acharya, and P. Bhat. “Removal of Crystal Violet dye from aqueous solution using water hyacinth: Equilibrium, kinetics and thermodynamics study.” Resource-Efficient Technologies, 3:71-77, 2017.

[16] G.K. Sarma, S.S. Gupta, and K.G. Bhattacharyya. “Adsorption of Crystal violet on raw and acid-treated montmorillonite, K10, in aqueous suspension.” Journal of Environmental Management, 171, pp.1-10, 2016.

[17] P. Sharma and H. Kau. “Sugarcane bagasse for the removal of erythrosin B and methylene blue from aqueous waste, ”Applied Water Scienc, 1, pp.135–145, 2011.

[18] J. Shi, D. Xing, and J. Li, “FTIR “Studies of the Changes in Wood Chemistry from Wood Forming Tissue under Inclined Treatment.” Energy Procedia, 16, pp.758-762, 2012.

[19] H.N. Tran, S.J. You and H.P. Chao, “Insight into adsorption mechanism of cationic dye onto agricultural residues-derived hydrochars: Negligible role of π-π interaction,” Korean J. Chem. Eng, 34(6), pp.1708-1720, 2017

[20] Q.-X. Liu, Y.-R. Zhou, M. Wang, Q. Zhang, T. Ji, T.-Y. Chen and D-C. Yu, “Adsorption of methylene blue from aqueous solution onto viscose-based activated carbon fiber felts: Kinetics and equilibrium studies,” Adsorption Science & Technology, pp. 1-21, 2019.

[21] P. S. Kumar, S. Ramalingam, C. Senthamarai, M. Niranjana, P. Vijayalakshmi, and S. Sivanesan, " Adsorption of dye from aqueous solution by cashew nut shell: Studies on equilibrium isotherm, kinetics and thermodynamics of interactions," Desalination, 261, pp. 52–60, 2010.

[22] S. M. Yakout and E. Elsherif, " Batch kinetics, isotherm and thermodynamic studies of adsorption of strontium from aqueous solutions onto low cost rice-straw based carbons," Carbon-Science and Technology, 3, pp. 144 – 153, 2010.

[23] K. M. Doke, M. Yusufi, R. D. Joseph and E. M. Khan, "Comparative Adsorption of Crystal Violet and Congo Red onto $ZnCl_2$ Activated Carbon," Journal of Dispersion Science and Technology, 37(11), pp.1671–1681, 2015.

[24] A. Nath, S. Chakraborty and C. Bhattacharjee, "Bioadsorption of industrial dyes from aqueous solution onto water hyacinth (Eichornia crassipes): equilibrium, kinetic and sorption mechanism study," Desalination and Water Treatment, pp.1-11, 2013, doi: 10.1080/19443994.2013.787028

[25] S. Kaur, S. Rani, and R.K. Mahajan, "Adsorption Kinetics for the Removal of Hazardous Dye Congo Red by Biowaste Materials as Adsorbents," Journal of Chemistry, Online. ID 628582, pp.1–12, 2013.

[26] N.A. Rashidi, S. Yusup and A. Borhan, "Isotherm and Thermodynamic Analysis of Carbon Dioxide on Activated Carbon," Procedia Engineering, 148, pp.630-637, 2016.

[27] I. Loulidi, F. Boukhlifi, M. Ouchabi, A. Amar, M. Jabri, A. Kali, S. Chraibi, C. Hadey and F. Aziz, "Adsorption of Crystal Violet onto Agricultural Waste Residue: Kinetics, Isotherm, Thermodynamics, and Mechanism of Adsorption," The Scientific World Journal, 2020, Article ID 5873521, 9 pages, http//doi.org/10.1155/2020/5873521

[28] H.N. Tran, Y.F. Wang, S.J. You and H.P. Chao, "Insights into the mechanism of cationic dye adsorption on activated charcoal: The importance of π-π interactions," Process Safety and Environmental Protection, 107, pp. 168-180, 2017.